

Ab Initio Study of the Intra- and Intermolecular Bonding in AuCl(CO)[†]

Alessandro Fortunelli*

Istituto di Chimica Quantistica ed Energetica Molecolare (ICQEM) del CNR, Via V. Alfieri 1, I-56010 Ghezzano (PI), Italy

Guido Germano

H. H. Wills Physics Laboratory, University of Bristol, Tyndall Avenue, Bristol BS8 1TL, United Kingdom

Received: March 15, 2000; In Final Form: September 12, 2000

The intra- and intermolecular bonds in AuCl(CO) are investigated at the Hartree–Fock, density functional and second-order Møller–Plesset levels using a triple- ζ -valence-plus-polarization basis with effective core potentials and two additional f -type functions on the gold atom. Calculations on molecular fragments, the AuCl(CO) molecule, and a head–tail [AuCl(CO)]₂ dimer are compared with experimental data of vibrational frequencies and interatomic distances in the crystal. Insight is gained on the nature of the bonding in these type of complexes, especially the elusive intermolecular interaction. For the monomer, the extent of σ -donation and π -back-donation in the Au–(CO) interaction is analyzed in detail. For the dimer, the good agreement between the solid-state structure and the simple head–tail model suggests that the crystal geometry is due primarily to electrostatic interactions, though a more elaborate analysis of the charge density reveals also weak covalent Au–Au and C–Cl bonds.

1. Introduction

An accurate theoretical description of the bonding involving transition metal atoms is of fundamental importance for the modeling of phenomena in organometallic chemistry, surface and material science, and catalysis. In this context, considerable attention has been devoted to studying species exhibiting intermolecular M···M contacts in view of the possibility of developing metallic-type interactions within an otherwise organometallic environment. The quantum chemical description of transition metal compounds is not an easy task and requires the explicit treatment of electron correlation and relativistic effects. Density functional and post-Hartree–Fock calculations at the scalar relativistic level represent convenient alternatives for the treatment of such effects. However, comparisons between the results derived within the two classes of approach and available experimental data, or utilizing different exchange-correlation functionals, or studying the convergence of the results with respect to the choice of the basis set, are not frequent in the literature, despite the fact that they would be required in order to assess the accuracy of the theoretical methodology. In the present article we report a theoretical analysis of intra- and intermolecular interactions in AuCl(CO), a species that has been known for a long time¹ and that has recently been the subject of renewed experimental² and theoretical³ interest. Attention has been paid to make the approach as numerically reliable as possible and to compare the results of different methodological approaches. The aims of this work are (a) to analyze the isolated AuCl(CO) molecule in terms of molecular fragments and find the main intramolecular interactions (for example, to what extent Au π -back-bonds to CO, or is the carbon atom positively or

negatively charged?); (b) to investigate the main intermolecular interactions when two AuCl(CO) molecules approach (i.e., Au···Au and/or C···Cl); and (c) to elucidate the character of such intermolecular interactions and determine to what extent they affect the geometry of the system and the intramolecular interactions. The results of the simple dimer model will also be compared with the experimental data on the crystal. These issues will be studied on a particular system, but are of a fundamental nature that interests an entire class of transition metal complexes.

2. Approach

Three theoretical methods have been used in this study: the Hartree–Fock (HF) method, which is an independent electron model, and two approaches that take electron correlation into account along two alternative paths, specifically (a) a post-HF method at the level of Møller–Plesset second-order perturbation theory (MP2) and (b) a density functional (DF) method that utilizes the functional of Perdew and Wang⁴ for both exchange and correlation (PW91–PW91). Within these three approaches, the structure of the basic AuCl(CO) unit (a “monomer”) has first been optimized in the gas phase together with those of a few related molecules: CO, AuCl and Au(CO)⁺.

Second, geometry optimizations have been performed for a hypothetical model system consisting of two AuCl(CO) units (a “dimer”), in which the atoms of each monomer were imposed to move along two parallel lines that were kept at the distance experimentally observed between the molecular axes in crystalline AuCl(CO); in other words, $d = 3.35 \text{ \AA}$.⁵

Two different optimizations have been performed in the dimer case. In the first (“unconstrained”) optimization, hereinafter referred to by adding the suffix “u” to the acronyms identifying each method (HFu, DFu, MP2u), no further geometrical constraint has been imposed. In the second (“constrained”) optimization, hereinafter referred to by adding the suffix “c” to

[†] Dedicated to Prof. Fausto Calderazzo on the occasion of his 70th birthday.

* Corresponding author. Tel.: +39-050-3152 447. Fax: +39-050-3152 442. E-mail: A.Fortunelli@icqem.pi.cnr.it.

the acronyms identifying each method (HFc, DFc, MP2c), the intramolecular distances within each monomer were forced to coincide with those derived from the experimental crystalline structure:⁵ $R(\text{AuCl}) = 2.261 \text{ \AA}$, $R(\text{AuC}) = 1.930 \text{ \AA}$, $R(\text{CO}) = 1.11 \text{ \AA}$. The goal was to elucidate the modifications imposed on the monomer structure by dimerization (as the first hypothetical step in the process of crystal formation) and to characterize the type and strength of the intermolecular interactions in this system. To this aim, the electron density of the various molecular species has been analyzed through the Mulliken, electrostatic potential fit (ESP),⁶ natural bonding orbital (NBO),⁷ and Bader⁸ methods. NBO theory has also been used to perform a second-order perturbative analysis of intramolecular energy interactions.

3. Computational Details

The ab initio HF, DF, and MP2 calculations were performed using the GAUSSIAN 94⁹ and GAUSSIAN 98¹⁰ sets of programs on DEC workstations at ICQEM in Pisa and on an SGI Origin 2000 at the H. H. Wills Physics Laboratory in Bristol. A basis set of triple- ζ -valence-plus-polarization (TZVP) quality¹¹ was employed, which uses pseudopotentials¹² and incorporates spin-orbit averaged relativistic effects for the gold atom. Two additional uncontracted f -type Gaussian functions were added onto the gold atom, with exponents 2.5 and 1.447.¹³ The options in the GAUSSIAN program were set so that the numerical accuracy of the calculations should be better than 0.1 kcal/mol. No excitations from the $1s^2$ core of carbon and oxygen and the $1s^2 2s^2 2p^6$ core of chlorine were included in the MP2 calculations. Despite the lack of Darwin and mass-polarization relativistic corrections in the pseudopotentials, the present computational approach should describe the energetics of the atom-atom interactions in this system reasonably well. NBO and ESP analyses are supported by GAUSSIAN. The Bader analysis, not supported by GAUSSIAN 94, was performed at the simplest possible level through direct inspection of plots of the total electron density in the plane of the system and with software of our own that reads density grid output by GAUSSIAN, locates the critical points, evaluates the Hessian numerically, and diagonalizes it as described later in the text. The density contour plots in Figure 2 have been realized with PV-WAVE.

4. Results and Discussion

Monomer: Structure. Let us first consider the results of the three theoretical methods on the basic (monomer) unit. The values of the optimized distances, the dipole moment and the harmonic vibrational frequencies for CO, AuCl, Au(CO)⁺, and AuCl(CO) are reported in Table 1, together with the values of the gross Mulliken charges. In the following, charges derived through more sophisticated approaches, such as an ESP fit using the atomic radii $R(\text{Au}) = 2.0 \text{ \AA}$, $R(\text{Cl}) = 1.7 \text{ \AA}$, $R(\text{C}) = 1.5 \text{ \AA}$ and $R(\text{O}) = 1.4 \text{ \AA}$, or the NBO theory, will also be reported. In the present calculations, the Mulliken analysis does not give absolute values but relative trends usually in fair agreement with those of the other approaches. Moreover, the NBO analysis predicts an unreasonably large charge separation for the CO molecule, while the ESP values for the charges on the central atoms of the AuCl(CO) molecule cannot be directly utilized to give an idea of the charge distribution within the monomer (see below the discussion following Table 4). Mulliken charges have therefore been reported, see Table 1. From an inspection of this table, some differences in the theoretical description of these species emerge.

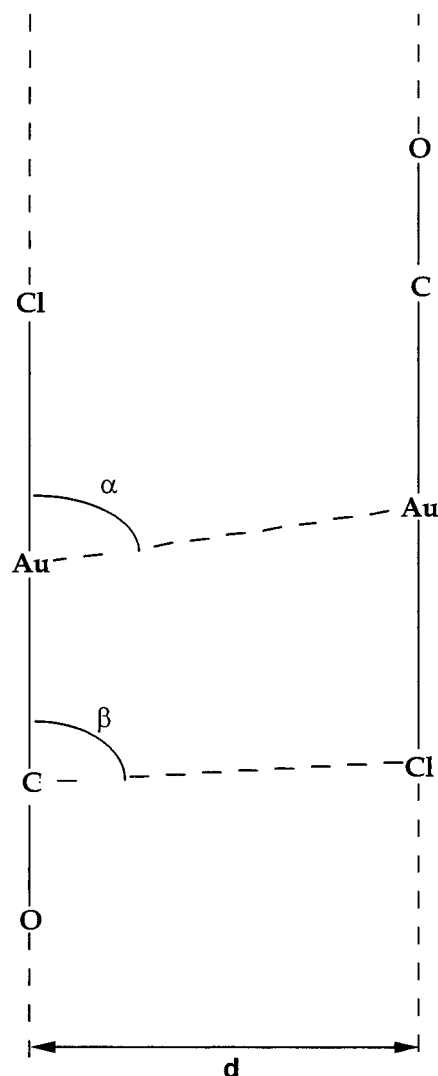


Figure 1. Structure of the dimeric unit $[\text{AuCl}(\text{CO})]_2$. The distance $d = 3.35 \text{ \AA}$ is taken from X-ray data.⁵ In the figure, the angles α and β are also defined.

Because it is known that the method has serious limitations in describing this kind of system, the HF results have been reported essentially for reference reasons and in connection with “hybrid” density functional approaches (see below). In particular, the peculiar electronic structure of the CO molecule is badly missed (wrong sign of the dipole moment and largely overestimated harmonic frequency). Similar considerations apply to the interaction of CO with Au⁺ in Au(CO)⁺, for which the HF approach predicts a negligible dipole moment μ (to be compared with an estimated value larger than 3 D) and a harmonic frequency for the Au-C stretching probably off by a factor of ~ 1.7 . As expected, the Au⁺-Cl⁻ interaction in AuCl is better described. However, the dipole moment and charge separation between the two atoms are appreciably overestimated. In passing, it can be noted that the Au⁺-Cl⁻ interaction, though formally corresponding to an ionic bond, bears a charge separation that is far from being complete. This can be explained on the basis of the values of the ionization potentials and electron affinities of the involved atoms: $\text{IP}(\text{Au}) = 9.22 \text{ eV}$ and $\text{EA}(\text{Cl}) = 3.61 \text{ eV}$.

The DF results, instead, compare reasonably well with the MP2 results. In particular the optimized distance, the dipole moment, the charge separation and the harmonic vibrational frequency of CO are correctly reproduced with only minor

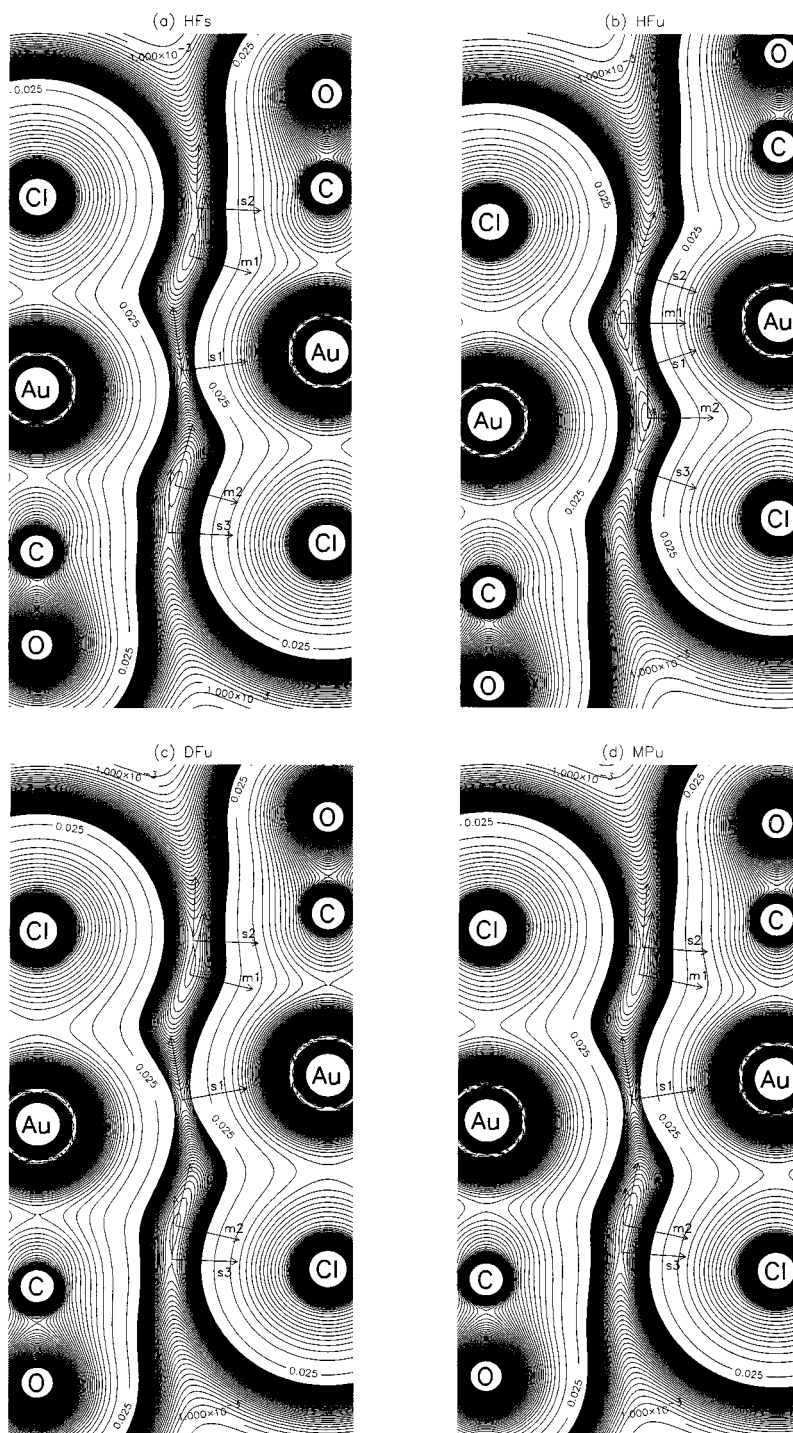


Figure 2. Contour plots of the total electron density (in $e/\text{\AA}^3$) for the dimeric unit of $\text{AuCl}(\text{CO})$, as obtained from several theoretical methods: HF_s, HF_u, DF_u, and MP_u (see text for definition). In correspondence with the intermolecular (3,−1) (s1,s2,s3), and (3,+1) (m1,m2) critical points, the eigenvectors of the Hessian of the density are plotted as arrows normalized to an arbitrary length of 0.75 Å. The density hole around each gold nucleus is due to a pseudopotential, that allows to neglect the core electrons in the calculations. Isodensity lines were plotted every 0.025 units, and additionally every 0.00025 units up to 0.015 units to capture the low density in the intermolecular region. The graph is 4.0×8.0 Å wide; the radius of the white area containing each atomic label is 1/8 of the radius used for the ESP fit of that atom. The HF_s, DF_u, and MP_u plots show one Au–Au (s1) and two C–Cl (s2,s3) saddle points, corresponding to chemical bonds, separated by two local minima (m1,m2); however, if the HF_s structure is left free to relax to its unconstrained geometrical optimum HF_u, the C–Cl saddle points are substituted by Au–Cl saddle points.

differences. The same applies to the $\text{Au}^+-(\text{CO})$ interaction in $\text{Au}(\text{CO})^+$, even though in this case there is a tendency to overestimate the strength of the Au–C bond (π -back-bonding interaction), which produces a larger “Au–C” harmonic frequency. The slightly larger increase in the “C–O” stretching frequency with respect to the CO molecule can probably be explained in terms of a stronger effect of the electric field of

the Au^+ fragment at the DF level.¹⁴ Moreover, it is well known that the DF approach tends to underestimate the strength of the atom–atom interaction in ionic species such as AuCl . The charge separation and the vibrational frequency are underestimated, whereas the bond distance is overestimated. For comparison, the experimental Au–Cl harmonic frequency is 382.8 cm^{-1} .¹⁵ Contrary to what might be expected, the description of

TABLE 1: Values of Optimized Distances (R), Dipole Moments (μ), Mulliken Charges (Q), and Harmonic Vibrational Frequencies (ω) for Selected Molecules Reported as Derived from *ab Initio* Calculations and Compared with Available Experimental Data for CO from ref 15^a

system	method	R(AuCl)	R(AuC)	R(CO)	μ	Q_{Au}	Q_{Cl}	Q_{C}	Q_{O}	ω
CO	HF			1.104	-0.19			0.19	-0.19	2441.3
	DF			1.137	0.17			0.03	-0.03	2138.9
	MP2			1.139	0.28			0.05	-0.05	2128.7
	exp			1.128	0.112					2169.8
	HF	2.328			6.28	0.53	-0.53			328.3
ClAu	DF	2.262			3.37	0.26	-0.26			336.6
	MP2	2.224			4.30	0.34	-0.34			381.8
	HF		2.179	1.090	-0.27	0.90		0.18	-0.08	229.1, 276.3(π), 2572.4
AuCO ⁺	DF		1.915	1.129	-3.28	0.77		0.16	0.07	306.8(π), 416.4, 2216.3
	MP2		1.919	1.131	-3.29	0.84		0.08	0.08	321.2(π), 389.3, 2192.5
	HF	2.307	2.030	1.098	6.66	0.42	-0.48	0.22	-0.16	79.6(π), 308.1, 361.6, 379.9(π), 2496.4
ClAuCO	DF	2.265	1.898	1.144	3.65	0.24	-0.27	0.09	-0.07	72.2(π), 363.4, 417.8(π), 456.1, 2114.9
	MP2	2.251	1.864	1.142	4.72	0.35	-0.34	0.04	-0.05	78.6(π), 386.0, 439.4(π), 473.1, 2123.6

^a Distances are given in Å, dipole moments in Debye, frequencies in cm⁻¹ and charges in atomic units.

TABLE 2: Differences between the Natural Atomic Orbital (NAO)⁷ Electron Populations in the AuCl(CO) Molecule with Respect to Those in the Parent CO and AuCl Molecules, According to the DF and MP2 Approaches^a

atom	Δq		$\Delta q_{s\sigma}$		$\Delta q_{p\sigma}$		$\Delta q_{p\pi}$		$\Delta q_{d\sigma}$		$\Delta q_{d\pi}$	
	DF	MP2	DF	MP2	DF	MP2	DF	MP2	DF	MP2	DF	MP2
Au	-0.07	-0.02	0.24	0.29	0.00	0.01	0.00	0.00	-0.05	-0.08	-0.26	-0.24
Cl	0.10	0.09	-0.02	-0.02	0.20	0.15	-0.08	-0.04	0.00	0.00	0.00	0.00
C	0.06	0.05	-0.36	-0.33	0.05	0.05	0.37	0.33	0.00	0.00	0.00	0.00
O	-0.10	-0.11	-0.03	-0.03	-0.02	-0.02	-0.05	-0.06	0.00	0.00	0.00	0.00

^a The NAO population differences (in atomic units of charge) are given as total charge drift: Δq , and further distinguished according to the orbital symmetries: $s\sigma$, $p\sigma$, $p\pi$, $d\pi$ and $d\sigma$, where σ and π label the axial symmetry, while s, p and d label the atomic origin.

the ionic interaction is not improved (from trial calculations not reported here) by passing to other exchange functional forms, such as the Becke¹⁶ or the modified Perdew–Wang (MPW)¹⁷ form. The use of the Lee–Yang–Parr¹⁸ functional for correlation is not helpful either; on the contrary, it uniformly deteriorates the quality of the results. On the other hand, the introduction of a small percentage of the HF exchange into the density functional, i.e., by considering a so-called “hybrid” method in the form of the MPW1–PW91 functional¹⁷ improves the AuCl case. This result cannot be generalized because, for example, it does not apply to CuCl and it also badly describes the CO molecule, whose harmonic frequency is predicted to be ~ 80 cm⁻¹ larger than the experimental value. This is probably to be connected with the poor performance of the HF approach for the CO molecule (see above). We therefore decided to use the PW91–PW91 approach throughout.

The incorrect description of the AuCl interaction at the DF level reflects itself on the AuCl(CO) molecule, which is described worse than, for example, Au(CO)⁺. Not only is the total dipole moment smaller at the DF level than at the MP2 level, but also (a) the Au–C and C–O stretching modes are more intermixed, which explains the smaller increase in the “Au–C” stretching frequency with respect to Au(CO)⁺ and (b) the gold atom, being less positive, interacts more strongly with the carbonyl unit, inducing a larger charge separation on it. The tendency to overestimate the π -back-bonding interaction, already present in Au(CO)⁺, is more pronounced here. This can be seen by the larger decrease of the CO harmonic frequency from 2139 to 2115 cm⁻¹ at the DF level, to be compared with the smaller decrease at the MP2 level from 2129 to 2124 cm⁻¹, and from the larger absolute values of the Mulliken charges on the C and O atoms. These results compare reasonably well with those by Antes et al.³ both for the numerical values and the theoretical interpretation.

The dissociation energy of the AuCl(CO) molecule into AuCl and CO fragments is predicted to be 52.6 and 52.5 kcal/mol by

DF and MP2 approaches, respectively (zero-point vibrational corrections were not taken into account). These values are in good agreement with the experimental estimate of ≥ 50.2 kcal/mol in ref 2 and the MP2 theoretical calculation of 52.6 kcal/mol in ref 3. The dissociation energy into Au(CO)⁺ and Cl⁻ fragments is predicted to be 203.7 and 198.0 kcal/mol by DF and MP2 approaches, respectively (these numbers are decreased by 9.5 and 7.9 kcal/mol, respectively, if using a properly diffuse basis set to describe the Cl⁻ anionic fragment).

Monomer: Electron Density. It is interesting to analyze the results of the NBO approach on the molecular species discussed up to now. A comparison between the natural atomic orbital (NAO)⁷ populations in the AuCl(CO) molecule with those of the parent CO and AuCl molecules is particularly instructive and is reported in Table 2 for the DF and MP2 approaches. From an analysis of Table 2, the following points emerge.

At the DF level, the carbon atom σ -donates electron charge to the gold atom: $\Delta q_{s\sigma}(\text{C}) = -0.36$, $\Delta q_{s\sigma}(\text{Au}) = +0.24$, but at the same time the gold atom π -back-donates charge to the C atom: $\Delta q_{d\pi}(\text{Au}) = -0.26$, $\Delta q_{p\pi}(\text{C}) = 0.37$, so that the net charge drifts are small. In this respect, it can be noted that a similar gross Mulliken analysis gives a slightly increased electron population on the gold atom and a slightly decreased one on the carbon atom in passing from the CO and AuCl molecules to the AuCl(CO) complex. However, what matters here are the relative changes in the σ - and π -systems, which are much larger and, as such, unambiguous.

The Δq values at the MP2 level are comparable to the DF values, even though they confirm the tendency of the DF approach to (a) overestimate the Au–(CO) π -back-bonding interaction [see the smaller MP2 values for $\Delta q_{d\pi}(\text{Au})$ and $\Delta q_{p\pi}(\text{C})$] and (b) describe incorrectly the Au⁺–Cl⁻ interaction [see the values of $\Delta q_{s\sigma}(\text{Au})$ and $\Delta q_{p\sigma}(\text{Cl})$].

The presence of an appreciable π -back-donation from the gold atom to the CO molecule is further confirmed by an NBO analysis. At the DF level, for example, it is found that in the

TABLE 3: Values^a of Optimized Geometrical Parameters of AuCl(CO) Dimers Reported as Derived from Ab Initio Calculations or Experimental Data on the Crystal^b

method	AuCl	AuC	CO	Au...Au	C...Cl	Au...Cl	Au...C	Δ_{AuAu}	Δ_{ClC}	α	β
exp	2.261	1.930	1.11	3.380	3.352	3.808	4.111	0.451	0.122	82.3	87.9
DFu	2.286	1.910	1.141	3.402	3.357	3.754	4.181	0.591	0.216	80.0	86.3
MP2u	2.268	1.877	1.140	3.388	3.352	3.784	4.113	0.509	0.115	81.4	88.0
DFc	exp	exp	exp	3.387	3.354	3.784	4.141	0.502	0.176	81.5	87.0
MP2c	exp	exp	exp	3.375	3.351	3.826	4.089	0.412	0.081	83.0	88.6

^aThe angles α and β are defined in Figure 1. Distances are given in Å and angles in degrees.

AuCl(CO) molecule as much as 0.79 units of electronic charge cannot be described in terms of Lewis valence structures. About 0.71 are of valence type and are distributed as follows: 0.38 on the Au–C antibond $\sigma^*(\text{AuC})$, 0.32 on the (two) CO π -antibonds $\pi^*(\text{CO})$, and 0.015 on the σ -antibond $\sigma^*(\text{CO})$. For comparison, the π -back-donation in $\text{Au}(\text{CO})^+$ is found to be comparatively less important, with only 0.014 units of charge on $\sigma^*(\text{AuC})$, 0.18 on $\pi^*(\text{CO})$, and 0.014 on $\sigma^*(\text{CO})$.

At the MP2 level the situation is analogous, with the main difference being that the contribution from Rydberg orbitals is larger, as should be expected from an approach not based on a single determinant: 1.05 units of charge escape a single-structure representation, 0.74 of which are of valence type and are distributed as follows: 0.36 on $\sigma^*(\text{AuC})$, 0.34 on the (two) $\pi^*(\text{CO})$, and 0.04 on $\sigma^*(\text{CO})$.

Such a huge contribution from antibonding (non-Lewis-type-structure) orbitals to the molecular electron density in AuCl(CO) must reflect itself on the second-order energy lowering associated with bonding/antibonding interactions in the NBO energy analysis.⁷ In fact, at the DF level (for which an effective single-electron operator is available in the GAUSSIAN program) one finds that, whereas in the parent CO and AuCl compounds the donor–acceptor interactions are minor (to give an idea: only ~20 kcal/mol for the oxygen lone-pair or core orbitals with the carbon Rydberg orbitals in CO), in the AuCl(CO) molecule one encounters energy lowering of ~160 kcal/mol for the chlorine lone-pairs interacting with $\sigma^*(\text{AuC})$, ~192 kcal/mol for $\sigma^*(\text{AuC})$ interacting with carbon, oxygen or gold Rydberg orbitals, and finally ~33 kcal/mol for the gold lone-pairs interacting with the $\pi^*(\text{CO})$ orbitals. In contrast, this interaction is the most relevant one in $\text{Au}(\text{CO})^+$, where it amounts to ~27 kcal/mol.

These results are in good agreement with those by Antes et al.³ and nicely complement their analysis of σ -donation and π -back-donation in the AuCl–(CO) interaction.

Dimer: Structure. We now consider the theoretical results on the dimer system. The values of the optimized geometrical parameters derived from constrained and unconstrained calculations (as described in Section 2) are reported in Table 3, together with the available experimental data on crystalline AuCl(CO).⁵ The gold atom is linearly coordinated with the chlorine and carbon atoms, with a distance between two nearest-neighbor monomer axes of 3.35 Å. However, the vicinal gold atoms do not lie on the same plane (see ref 2 for a clear picture of the packing in the crystal), and it was suggested² that the C...Cl intermolecular contacts of 3.352 Å should be at least as important as the Au...Au contacts of 3.380 Å.

To investigate more deeply these issues, calculations have been performed on the dimeric unit shown in Figure 1, where the angles α and β are also defined, deviations from 90° giving a measure of the deviation of the closest approach between the Au...Au or C...Cl contacts, respectively. The projections of R(Au...Au) and R(C...Cl) onto the molecular axes are indicated as Δ_{AuAu} and Δ_{ClC} , respectively. A few of the geometrical

parameters given in Table 3 are clearly redundant, but have been reported for the sake of clarity.

A comparison between Table 1 and Table 3 shows that the DF and MP2 theoretical approaches predict similar changes in the interatomic distances following dimerization. The MP2 level, for example, gives a very small decrease of the CO bond length of 0.002 Å, and an increase of the AuCl and AuC bond lengths of 0.017 and 0.013 Å, respectively. Furthermore, the DF and MP2 unconstrained approaches seem to reproduce correctly the experimental solid-state values of Δ_{AuAu} , Δ_{ClC} , α and β , even though the optimization is limited to a dimeric unit only.

The agreement with the experimental structure is slightly improved in the constrained calculations, which, however, preserve a strong resemblance to the unconstrained calculations. At the MP2 level, for example, the requirement that the intramolecular distances be equal to the experimental distances essentially implies only a shorter C–O distance and a larger Au–C distance, and therefore a stronger C...Cl interaction.

The high stability of the molecular geometry with respect to selectively “un-constraining” structural degrees of freedom and the fact that the solid state structure can be predicted in a substantially correct way by considering a simple dimer model proves that our dimer approach correctly describes the basic intermolecular interactions in the solid. Furthermore, these facts also suggest that the AuCl(CO) geometry in the solid state is primarily determined by electrostatic (e.g., dipole–dipole) and exchange-repulsion interactions. The HF method accounts for such intermolecular forces, but assigns to each monomer an exceedingly large value of the dipole moment, thus precluding the possibility of a correct structural prediction, and indeed the HF calculations grossly overestimate the Δ_{AuAu} and Δ_{ClC} geometrical parameters. The DF approach, on the contrary, giving a more reasonable value for the dipole moment, also yields a reliable description of the dimerization process.

This is confirmed by a simple model calculation. In Table 4, the values of the ESP atomic charges for the monomers and unconstrained dimers are reported as derived from DF and MP2 calculations. The ESP charges are optimized to reproduce the electrostatic potential of the molecule outside the van der Waals region. One can therefore consider a simple model in which these charges are placed on the positions of the corresponding atoms (chosen according to the proper theoretical method) along the two parallel lines previously defined, and limit the optimization to the relative position of the two “monomer units”. At the DF level, then, one finds an electrostatic interaction energy of –3.6 kcal/mol when using the monomer ESP charges and distances, and –4.4 kcal/mol when using the dimer values; the latter give larger interaction energies because they account for the mutual polarization of the monomers. The DF-optimized Δ_{AuAu} and Δ_{ClC} geometrical parameters are 0.826 and 0.459 Å, respectively, in the former case, and 0.746 and 0.370 Å, respectively, in the latter case. The geometrical parameters so derived compare reasonably well with those obtained through a full optimization, see Table 3. The MP2 values of the

TABLE 4: Atomic Charges on Monomer (m) AuCl(CO) and Unconstrained Dimer (d) [AuCl(CO)]₂ Molecules According to the Mulliken, ESP,⁶ and NBA⁷ Analyses and from HF, DF, and MP2 Calculations^a

method	Mulliken				ESP				NBA			
	Au	Cl	C	O	Au	Cl	C	O	Au	Cl	C	O
DF												
m	0.242	-0.267	0.094	-0.070	-0.012	-0.219	0.379	-0.147	0.477	-0.518	0.384	-0.343
d	0.235	-0.290	0.113	-0.057	-0.010	-0.242	0.376	-0.124	0.467	-0.544	0.411	-0.335
MP2												
m	0.352	-0.339	0.042	-0.055	0.034	-0.286	0.360	-0.108	0.515	-0.580	0.366	-0.302
d	0.331	-0.363	0.070	-0.038	0.025	-0.306	0.368	-0.086	0.495	-0.600	0.393	-0.289

^a All values in atomic units of charge.

geometrical parameters are similar to the DF ones: 0.872 (0.752) Å and 0.485 (0.361) Å, respectively, in the monomer (dimer) case, whereas the interaction energies are somewhat larger: -5.3 (-6.3) kcal/mol when using the monomer (dimer) charges and distances. It can be noted that the HF results for the geometrical parameters are substantially overestimated and become worse in passing from the monomer to the dimer data (the electrostatic interaction energy is already overestimated and further increases when polarization effects are included). For later use, the HF electrostatic dimerization energy reads -11.7 kcal/mol.

From the ESP values in Table 4, it is apparent that the electrostatic interaction between the AuCl(CO) molecules can be roughly modeled as an attraction between the negatively charged chlorine atom and the positively charged carbon atom, counterbalanced by a repulsion with the negatively charged oxygen atom.

The residual nonelectrostatic intermolecular interactions, i.e., essentially exchange-repulsion, dispersion, and weakly covalent interactions, thus apparently give a minor contribution to the overall atomic arrangement, even though they influence the total dimerization energy, which is found to be -8.2, -5.2, and -8.8 kcal/mol at the HFu, DFu, and MP2u levels, respectively. Exchange-repulsion interactions tend to *increase* the value of Δ_{AuAu} , and this is indeed the case for the HF approach (which additionally accounts only for such interactions). The HFu values of Δ_{AuAu} are *larger* than those derived from the simple electrostatic model. On the contrary, dispersion and covalent interactions tend to *decrease* Δ_{AuAu} , and, in fact, at the DFu and MP2u levels they eventually overcome the repulsion due to exchange forces, thus producing values of Δ_{AuAu} that are appreciably *smaller* than those derived from the simple electrostatic model.

It is difficult to give a quantitative estimate of the energy associated with nonelectrostatic effects. The repulsive interactions can be estimated as the difference between the dimerization energies of the HFu approach and of the simple electrostatic model using HFu values for charges and distances, i.e., about 3.5 kcal/mol. The electrostatic energy curve and the full HF curve are very *smooth* around their minimum, with differences between the various relative positions of the monomer units of just a few tenths of a kcal/mol. The corresponding interactions are not strongly directional, and little information can be gained on the strength of the attractive interactions. However, these can be estimated as the difference between the MP2u dimerization energy (-8.8 kcal/mol from above) and the energy calculated at the HF level, but using the MP2-optimized distances (which turns out to be -6.4 kcal/mol), so that the final result is approximately -2.4 kcal/mol. The dispersion and covalent interactions thus represent a small but nonnegligible fraction of the total dimerization energy.

In passing, it may be noted that the DF approach, in contrast to the MP2 approach, cannot account in principle for dispersion interactions.¹⁹ The fact that the DFu dimerization energy is

comparable to the MP2u energy is therefore due to an underestimation of the exchange-repulsion forces and/or to an overestimation of the covalent forces. The reasonable results of the DF approach in this case are thus probably assured by a partial cancellation of errors.

Covalent interactions, even though they are not primarily important for determining the structural arrangement, are expected to appreciably influence the fine details of the electronic distribution. It is therefore interesting to analyze the electronic density of the dimeric unit in more detail, to see whether the qualitative picture of intermolecular interactions may emerge differently from the three methods.

Dimer: Electron Density. The predicted atomic charges for the monomers and unconstrained dimers are reported in Table 4 as derived from DF and MP2 calculations according to the Mulliken, ESP, and NBA methods. From an analysis of Table 4, it is possible to fix some common features of the effect of the dimerization process onto the atomic populations: (a) the chlorine atom acquires ~0.02 atomic units of charge and the oxygen atom loses 0.01–0.02 from both the DF and MP2 calculations and the three population analyses; (b) the Mulliken and NBO analyses give comparable results from the DF and MP2 approaches also for the other atoms: the carbon atom loses 0.02–0.03, whereas the gold atom acquires ~0.02 at the MP2 level and ~0.01 at the DF level; (c) the ESP analysis gives substantially different results for the gold and carbon atoms according to the DF method. With respect to the two other analyses, the charge differences following dimerization are smaller and have opposite signs on the two atoms; the MP2 approach gives smaller values for these charge differences.

Point (c) can be explained by considering that the ESP charges are intended to reproduce the electrostatic potential *outside* the molecular region, and the charges on the central atoms are very sensitive to this requirement. In fact, the Mulliken and ESP charges are similar for the AuCl molecule, in which case they roughly correspond to the value of the dipole moment divided by the interatomic distance, but the charge density and thus the electrostatic potential generated by it are appreciably deformed when the AuCl–CO adduct is formed, even though there is no large net charge drift between the two fragments, and this must reflect in the values of the ESP charges. Points (a) and (b), instead, can be easily interpreted in terms of a C...Cl "ionic" interaction, which leaves electronic charge on the gold atom free for a (presumably) covalent Au...Au interaction.

The development of the C...Cl intermolecular interaction also produces a weakening of the Au–(CO) σ - and π -back-bonding interaction. To give an idea, at the DF level the contribution of the non-Lewis-type structures decreases from 0.71 to 0.67 units of charge, distributed as follows: 0.37 on $\sigma^*(\text{AuC})$ and 0.28 on the two $\pi^*(\text{CO})$. Consequently, the CO bond re-enforces, and in fact one finds an increase in the harmonic CO stretching frequency from 2115 to 2129 cm⁻¹. This is confirmed also by the second-order NBO energy analysis: the interaction of the

gold core and lone-pairs with the $\pi^*(\text{CO})$ orbitals decreases by ~ 2.5 kcal/mol, whereas the interaction of the chlorine lone-pairs with $\sigma^*(\text{AuCl})$, and of $\sigma^*(\text{AuCl})$ with the carbon, oxygen, and gold Rydberg orbitals decreases by about 10–15 kcal/mol each.

The subtle differences that have been singled out through the various population analyses become more apparent when a more refined theoretical tool, such as the Bader analysis, is employed to compare the results of the different theoretical methods. Indeed, the Bader approach gives a more complete and interesting landscape for this process.

Figure 2 shows plots of the total electron density in the molecular plane for the dimeric $[\text{AuCl}(\text{CO})]_2$ unit as derived from HF (where “s” stands for “single point”, i.e., without optimization with respect to the crystallographic structure), HFu, DFu, and MP2u calculations. The critical points of the density have been detected numerically, and the eigenvectors of the Hessian matrix of these points have been plotted as arrows. From an inspection of Figure 2, the differences in the description of the intermolecular interactions according to the three methods clearly appear.

The HF, DFu, and MP2u plots show one Au–Au and two C–Cl saddle points, corresponding to weak chemical bonds, separated by two local minima. However, when the HF structure is left free to relax to its unconstrained geometrical optimum (HFu), the C–Cl saddle points are substituted by Au–Cl saddle points. This qualitative difference between constrained and unconstrained calculations is peculiar to the HF method: instead, the plots of the DFs, MP2s, DFc, and MP2c electron densities are very similar to the corresponding DFu and MP2u densities, and, not being particularly informative, have not been reproduced. In this connection, it is interesting to note that both MPW–PW91 and MPW1–PW91¹⁷ unconstrained optimizations fail to reproduce the C–Cl bond.

It can also be noted that the DFu and MP2u plots resemble each other: the Au–Au and C–Cl saddle points are qualitatively similar, even though the former appears stronger than the latter, confirmed by the fact that it survives in conditions for which the other disappears. To put things on a quantitative basis, the values of the density and the Laplacian are ~ 0.014 $e/\text{\AA}^3$ and ~ 0.14 $e/\text{\AA}^5$, respectively, at the s1 critical point, and ~ 0.0075 $e/\text{\AA}^3$ and ~ 0.08 $e/\text{\AA}^5$, respectively, at the s2 critical point, from both MP2 and DF calculations.

The HF method performs even worse with a basis of lower quality, like the double- ζ -valence LanL2DZ:²⁰ the Au–Au saddle point disappears completely, and only two Au–Cl saddle points separated by a deep minimum are left. Also, the DF method misses the C–Cl saddle points when using this basis set, and only the MP2 method yields the same qualitative results. On the other hand, increasing the basis to TZVPP quality (i.e., adding a double set of polarization functions)¹¹ did not cause further improvements with respect to the augmented TZVP basis set utilized in the current approach, so that we are confident in its numerical stability.

In passing, from an inspection of Figure 2 one can derive values of atomic radii slightly different from those commonly utilized. For example, by taking the value of the radius as the point at which the electron density equals 0.015 $e/\text{\AA}^3$ and multiplying it by a factor of 1.2 (a common choice in the literature), one gets $R(\text{Au}) = 1.89$ \AA , $R(\text{Cl}) = 1.74$ \AA , $R(\text{C}) = 1.44$ \AA , and $R(\text{O}) = 1.37$ \AA . Using these values in the ESP analysis, however, does not qualitatively modify the previous conclusions.

It may also be noticed that the experimental crystalline value $R(\text{CO}) = 1.11$ \AA used in the constrained dimer calculations seems unrealistically low when compared with the experimental C–O distance of 1.1283 \AA in a free CO molecule¹⁵ because it would imply a very strong solid-state effect, and might therefore be ascribed to inaccuracies in the experimental data. In any case, test calculations in which this distance was let free to relax showed negligible differences in the intermolecular interactions, and this effect was not considered any further.

As a concluding remark, we underline the new insight gained in the present study on the nature of the elusive intermolecular bonding in this type of complexes. While the previous experimental literature on the subject was limited to qualitative considerations on experimental bond lengths and IR frequencies, a detailed analysis of the electronic structure was produced here, showing that there are indeed weak but quantifiable Au–Au and C–Cl covalent interactions. Before this work, the strength and even the presence of such covalent bonds were completely hypothetical.

Acknowledgment. We gratefully acknowledge Prof. Fausto Calderazzo, Prof. Daniela Belli Dell’Amico, and Prof. Fabio Marchetti for many enlightening discussions and useful suggestions; the Italian Consiglio Nazionale delle Ricerche (CNR) and the British Engineering and Physical Sciences Research Council (EPSRC) for financial support; Prof. Michael P. Allen (H. H. Wills Physics Laboratory, Bristol) for allowing the use of his computer resources; Andrea Biagi (ICQEM, Pisa), and Dr. Ian Stewart (Computer Centre, University of Bristol) for technical help.

References and Notes

- (1) Machot, W.; H. Gall, *Chem. Ber.* **1925**, *58*, 2175.
- (2) Belli Dell’Amico, D.; Calderazzo, F. *Gold Bulletin* **1997**, *30*, 21.
- (3) Antes, I.; Dapprich, S.; Frenking, G.; Schwerdtfeger, P. *Inorg. Chem.* **1996**, *35*, 2089.
- (4) Perdew, J. P.; Burke, K.; Wang, Y. *Phys. Rev. B* **1996**, *54*, 16533.
- (5) Jones, P. G. *Naturforsch.* **1982**, *37*, 823.
- (6) Besler, B. H.; Merz, K. M., Jr.; Kollman, P. A. *J. Comput. Chem.* **1990**, *11*, 431.
- (7) NBO Version 3.1, Glendening, E. D.; Reed, A. E.; Carpenter, J. E.; Weinhold, F. For a deeper discussion of this approach, see for example: Reed, A. E.; Curtiss, L. A.; Weinhold, F. *Chem. Rev.* **1988**, *88*, 899.
- (8) Bader, R. F. W. *Atoms in Molecules: A Quantum Theory*, Oxford University Press: Oxford, 1990.
- (9) *Gaussian 94, Revisions B.3 and D.4*, Frisch, M. J.; Trucks, G. W.; Schlegel, H. B.; Gill, P. M. W.; Johnson, B. G.; Robb, M. A.; Cheeseman, J. R.; Keith, T.; Petersson, G. A.; Montgomery, J. A.; Raghavachari, K.; Al-Laham, M. A.; Zakrzewski, V. G.; Ortiz, J. V.; Foresman, J. B.; Cioslowski, J.; Stefanov, B. B.; Nanayakkara, A.; Challacombe, M.; Peng, C. Y.; Ayala, P. Y.; Chen, W.; Wong, M. W.; Andres, J. L.; Replogle, E. S.; Gomperts, R.; Martin, R. L.; Fox, D. J.; Binkley, J. S.; Defrees, D. J.; Baker, J.; Stewart, J. P.; Head-Gordon, M.; Gonzalez, C.; Pople, J. A. Gaussian, Inc., Pittsburgh, PA, 1995.
- (10) *Gaussian 98, Revision A.6*, Frisch, M. J.; Trucks, G. W.; Schlegel, H. B.; Scuseria, G. E.; Robb, M. A.; Cheeseman, J. R.; Zakrzewski, V. G.; Montgomery, J. A., Jr.; Stratmann, R. E.; Burant, J. C.; Dapprich, S.; Millam, J. M.; Daniels, A. D.; Kudin, K. N.; Strain, M. C.; Farkas, O.; Tomasi, J.; Barone, V.; Cossi, M.; Cammi, R.; Mennucci, B.; Pomelli, C.; Adamo, C.; Clifford, S.; Ochterski, J.; Petersson, G. A.; Ayala, P. Y.; Cui, Q.; Morokuma, K.; Malick, D. K.; Rabuck, A. D.; Raghavachari, K.; Foresman, J. B.; Cioslowski, J.; Ortiz, J. V.; Stefanov, B. B.; Liu, G.; Liashenko, A.; Piskorz, P.; Komaromi, I.; Gomperts, R.; Martin, R. L.; Fox, D. J.; Keith, T.; Al-Laham, M. A.; Peng, C. Y.; Nanayakkara, A.; Gonzalez, C.; Challacombe, M.; Gill, P. M. W.; Johnson, B.; Chen, W.; Wong, M. W.; Andres, J. L.; Gonzalez, C.; Head-Gordon, M.; Replogle, E. S.; Pople, J. A. Gaussian, Inc., Pittsburgh, PA, 1998.
- (11) Schafer, A.; Huber, C.; Ahlrichs, R. *J. Chem. Phys.* **1994**, *100*, 5829. The exponents (included those of the polarization functions) and contraction coefficients can be retrieved from the following web-site: www.chemie.uni-karlsruhe.de/PC/TheoChem.
- (12) Andrae, D.; Haeussermann, U.; Dolg, M.; Stoll, H.; Preuss, H. *Theor. Chim. Acta* **1990**, *77*, 123.

- (13) Schwerdtfeger, P.; Bowmaker, G. A. *J. Chem. Phys.* **1994**, *100*, 4487.
- (14) Goldman, A. S.; Krough-Jespersen, K. *J. Am. Chem. Soc.* **1996**, *118*, 12159.
- (15) Huber, K. P.; Herzberg, G. "*Molecular Spectra and Molecular Structure: Constants of Diatomic Molecules*", Van Nostrand: NY, 1979.
- (16) Becke, A. D. *Phys. Rev. B* **1988**, *38*, 3098.

- (17) Adamo, C.; Barone, V. *J. Chem. Phys.* **1998**, *108*, 664.
- (18) Lee, C.; Yang, W.; Parr, R. G. *Phys. Rev. B* **1988**, *37*, 785.
- (19) Fortunelli, A.; Selmi, M. *J. Mol. Struct. (THEOCHEM)* **1995**, *337*, 25.
- (20) Hay, P. J.; Wadt, W. R. *J. Chem. Phys.* **1985**, *82*, 270. Wadt, W. R.; Hay, P. J. *J. Chem. Phys.* **1985**, *82*, 284. Hay, P. J.; Wadt, W. R. *J. Chem. Phys.* **1985**, *82*, 299.